Effect of Pressure and Temperature on the Thermal Conductivity of Rocks

Ilmutdin M. Abdulagatov,* Subkhanverdi N. Emirov, Zumrud Z. Abdulagatova, and Sabir Ya. Askerov

Institute for Geothermal Problems of the Dagestan Scientific Center of the Russian Academy of Sciences,
367003 Makhachkala, Shamilya Strasse 39-A, Dagestan, Russia

Effective thermal conductivity (ETC) of five dry rocks (sandstone, limestone, amphibolite, granulite, and pyroxene−granulite) have been measured over a temperature range from (273 to 423) K and at pressures up to 350 MPa with a steady-state parallel-plate apparatus. It is an absolute, steady-state measurement device with an operational temperature range of (273 to 1273) K and hydrostatic pressures up to 1500 MPa. The estimated uncertainty of the method is 2 %. The porosity of the samples (sandstone, limestone, amphibolite, granulite, and pyroxene−granulite) was 5 %, 5 %, 1.0 %, 1.0 %, and 1.2 %, respectively. A sharp increase of ETC was found for rocks at low pressures between (0.1 and 100) MPa along various isotherms between (273 and 423) K. At high pressures ($P >$ 100 MPa), a weak linear dependence of the ETC with pressure was observed. The measured values of ETC of rocks were used to test and confirm of applicability of the various theoretical and semiempirical models. The effect of structure (size, shape, and distribution of the pores), porosity, and mineralogical composition on temperature and pressure dependences of the ETC of various rocks types is discussed.

Introduction

Thermal conductivity is a key thermophysical property of rocks. In the earth's lithosphere, conduction of heat generally dominates among other mechanisms as radiation and advection. For estimations of crustal temperatures from heat flow and geothermal gradient data, the thermal conductivity of crustal layers and its dependence on temperature and pressure is need. Knowledge of temperature and pressure dependence of thermal conductivity, $\lambda(P, T)$, allows extrapolating to greater depths in order to estimate the temperature on the basis of well-founded data; therefore, such data are essential to model the thermal evolution of the earth's layers.[1,2] Recent geodynamic studies (geothermal modeling) show that the pressure and temperature dependence of the thermal conductivity controls many aspects of mantle convections.[3] Data on the variation of the thermal conductivity in the different layers of the earth is needed also to get the information at higher depth by numerically solving the heat transfer differential equations.[4−6] Luchenbruch and Sass[7] and Pribnow et al.[8] used rock thermal conductivity data and temperature gradients in the crust to estimates temperature down to several tens of kilometers based on data from the upper few kilometers. To develop the geothermal model of Earth (Earth's thermal field map), Čermak[5] used the temperature dependency of the thermal conductivity as $\lambda = \lambda_0(1 + AT)^{-1}$. To calculate of the local heat flow (heat flux, $Q = -\lambda(P, T)$-grad$T$, to identify subsurface heat flow fields) in the earth and localization of the superheated zones (heat flow anomalies), the values of thermal conductivity of cored samples of rocks as a function of temperature and pressure are also needed.[4,9,10] To increase the accuracy of the modeled temperatures distribution within the earth, more precise thermal conductivity data of rocks and rock-forming materials are required.[11]

Knowledge of the ETC of porous materials is of interest also to a wide range of engineers (heat containment, thermal rock working, electron beam drilling, artificial heating and cooling of buildings, weather control, drying of food grains, space technology, aviation, metallurgy, geothermal energy development techniques, etc.) and scientific applications involving heat transfer to or from various types of excavation. Thermal methods of oil recovery processes and shale oil retorting operations represent problems for which knowledge of the ETC of dry and fluid saturated porous media at high temperatures and high pressures is important.[12−15]

Determination of the ETC for rocks is a difficult problem because of the coupled nature of heat transfer phenomena in porous materials.[16] Therefore, the reported thermal conductivity data sets by various authors may vary significantly by as much as a factor of (2 to 3) for any given rock type. Even within the same rock type, thermal conductivity can vary over a considerable range. For a large number of rocks, thermal conductivity data are available and classified by rock name and origin in several extensive compilations.[17−23]

The main purposes of this study are (1) to provide accurate (estimate uncertainty of 2 %) experimental ETC data for geological porous materials (rocks) sandstone, limestone, amphibolite, granulite, and pyroxene−granulite with various porosities from (1 to 5) % at temperatures from (273 to 423) K and at pressures up to 350 MPa using a parallel-plate method, which has been used previously for accurate measurements on other solids and rock (dry and fluid-saturated) materials;[24−28] (2) to study the effect of temperature and pressure on the ETC behavior of dry rocks; and (3) to test the validity (applicability) of the various theoretical and semiempirical models for the prediction and calculation of the ETC of rocks as a function of temperature and pressure.

High Temperature and High-Pressure Thermal Conductivity Measurements of Rocks: Literature Review. The thermal conductivity of various rock types and rocks forming minerals at high temperatures and high pressures have been reported by many authors.[1,2,5,18,25−83] Basically the measurements of the ETC of rock materials reported in the literature were performed at high pressures but at low temperatures or at high temperatures

---

* Corresponding author present address: Physical and Chemical Properties Division, National Institute of Standards and Technology, 325 Broadway, Boulder, CO 80303. E-mail: ilmutdin@boulder.nist.gov. Fax: (303)497-5224. Tel: (303)497-4027.

10.1021/je050016a CCC: $33.50

and low pressures. The study of the combined effect of high temperature and high pressure on thermal conductivity of rocks is scarce. Mücke,[72] Ito et al.,[73] and Kiyohashi and Deguchi[74] reported the ETC data of unsaturated moist rocks: sandstone and shale, silt, tuff, and sandstone, respectively, at $T = 293$ K. Measurements were made with the hot-wire comparative method. Woodside and Messmer[71] measured the thermal conductivity for six consolidated sandstones using air, water, and heptane as pore saturants.

Buntebarth[1] performed measurements of the thermal conductivity of rock samples from a pilot well at temperatures up to 200 °C and at uniaxial pressures up to 60 MPa using heat flowmeter techniques. He found the effect of closure of pores and cracks on the thermal behavior of metabasites. Seipold and co-workers[29,30,37−41] used a pulse method to study the ETC and thermal diffusivity of rocks (amphibolite, granites) at high temperatures (up to 800 °C) and high pressures (up to 1000 MPa). Kukkonen et al.[42] used a transient method to measure the thermal conductivity of high-grade rocks at temperatures up to 1150 K and at pressures up to 1000 MPa. A decrease of (12 to 20) % in the thermal conductivity was found between room temperature and 1150 K, typical of phonon conductivity.

Horai and Susaki[43] made measurements of the ETC of silicate rock at temperatures from (300 to 700) K and at pressures up to 1200 MPa with an uncertainty of (4 to 5) % using a steady-state method. Huenges et al.[2] reported anisotropic thermal conductivities for 500 core samples. Measurements were made with a transient heat-flow method. The uncertainty of the measured values of thermal conductivity was about 5 %. Ljubimova et al.[58] reported the ETC of some sedimentary rocks and one sample of granite and andesite basalt at pressures up to 100 MPa. Popov et al.[64] and Popov and Romushkevich[65] used an optical scanning technique to measure the ETC for sedimentary rocks.

Thermal conductivity of dry and water-saturated low-porosity crystalline rocks (granitic samples) measured with a quick thermal conductivity meter at room temperature was reported by Schärli and Rybach.[66] Sass et al.[62] used two apparatus (USGS divided-bar, a steady-state comparative method, and the Shotherm “Quick Thermal Meter” (QTM), a transient strip heat source) to measure the ETC of rocks. The uncertainty of both devices was about 5 %. They reported ETC data for 17 specimens of most common rocks (andesite, basalts, sandstone, and granite). Schatz and Simmons[54] measured the ETC of several important earth materials in the temperature range from (500 to 1000) K. Birch and Clark[31] have measured the temperature and composition dependencies of the ETC of rocks.

Some researchers used an indirect method (thermal diffusivity measurements) of thermal conductivity measurements. The values of the thermal conductivity from thermal diffusivity measurement are defined as $\lambda = a\rho C_P$. The theoretical and experimental problems of the laser flash technique of the thermal diffusivity measurements has been discussed by Blumm and Lemarchand[84] and Blumm and Opfermann.[85] Osako and co-workers[76,77] simultaneously measured the thermal conductivity and the thermal diffusivity of garnet and olivine at pressures up to 8.3 GPa and at temperatures to 1100 K by using a pulse heating method. Xu et al.[86] calculated the lattice thermal conductivities from thermal diffusivity results using heat capacity and an equation of state for olivine, wadsleyite, and ringwoodite at temperatures up to 1373 K and at pressures to 20 GPa. Höfer and Schilling[79] reported thermal diffusivity data for quartz, orthoclase, and sanidine at elevated temperatures. Tommasi et al.[87] also measured the thermal diffusivity of mantle rocks between (290 and 1250) K. Chai et al.[88] reported the thermal diffusivity measurements of mantle minerals at high temperatures and high pressures.

Prediction and Correlation Techniques: Review. Since high-temperature and high-pressure measurements are difficult and since it is not possible to duplicate in the laboratory the conditions of the earth’s interior, theoretical and prediction methods can be used to extrapolate laboratory measurements to high temperatures and high pressures. This has been done by several authors.[54,69,75,78,89−91] The main difficulties in developing theoretical models to predict thermal conductivities for rocks are the complexities of the geometries of the rock structures. Due to irregularity of the microstructures, theoretical calculation of the ETC of porous materials, especially for fluid-saturated porous materials, is rather difficult and some times impossible. Existing prediction methods are based on certain simplifications such as parallel cylinders, spheres dispersed in a conducting medium, etc.[15,16,92−95] Even with a well-defined microstructure, the problem remains complex due to the existence of the interface resistance. A semiempirical approach is the only practical way of predicting the ETC of porous materials. Therefore, the models for calculating the ETC strongly depend on real material’s structure and microgeometry of dispersion. A large number of theoretical, semiempirical, and empirical models have been developed for the prediction of the ETC of multiphase porous materials.[15,16,51,53,74,92−101] An extensive review of literature on thermal conductivity models for rocks is performed by Somerton,[51] Odalevskii,[96] Mendel,[100] and Ljubimova et al.[102]

The ETC of rocks are affected by many factors, the most important being temperature, pressure, porosity, mineralogical composition, and microstructure. Walsh and Decker[46] and Beck[68] have developed a correlation equation for the estimating of the ETC of geological porous materials by a three-phase geometric mean model. The predicted values of the ETC agree with experiments within 22 %. Three different methods (numerical, predictive analytical, and bounds obtained by variation methods) for calculation of the ETC of composite porous materials were developed by Staicu et al.[101] The numerical calculations used the actual microstructure of the porous media. Recently, the semiempirical Debye’s model was developed by Giesting and Hofmeister[78] (based on the concepts of a phonon gas and damped harmonic oscillators) to calculate the thermal conductivity of garnets at ambient conditions with uncertainty of 6 %. The model was applied for natural (more complicated structures) mixed crystals with well-constrained chemical compositions. Giesting et al.[80] calculated the thermal conductivities of majoritic garnets at room temperature and pressure from infrared and Raman scattering data. They used a semiempirical model by Hofmeister[75] and Giesting and Hofmeister[78] to calculate the thermal conductivity for solid solutions from new measurements of their vibration spectra. The uncertainty in thermal conductivity determination is about (5 to 10) %.

At higher uniaxial pressure (above 100 MPa) the effect of pressure on ETC can be described with a linear relation:[19,29,33,42,43]

$$\lambda(P) = \lambda_0(1 + \alpha P) \tag{1}$$

where $\alpha = 1/\lambda_0(\partial\lambda/\partial P)_T$ is the pressure derivative (pressure coefficient), λ_0 is the reference thermal conductivity at zero pressure ($P = 0$). Zimmerman’s model,[15] an extension of the Maxwell model,[92] can be used to represent measured values of the ETC of low-porosity rocks. If the pores are assumed to be randomly oriented spheroids of aspect ratio (a), the parameter that characterizes the shape of a spheroid, and randomly distributed, the ETC has been given by Zimmerman:[15]

$$\frac{\lambda}{\lambda_S} = \left[\frac{(1-\phi)(1-b)+b\beta\phi}{(1-\phi)(1-b)+\beta\phi}\right] \tag{2}$$

where a is defined as the ratio of the length of the unequal axis to the length of one of the equal axes, M is a factor that depends on the aspect ratio of the pore a and $b \approx (0.001$ to $0.008)$ for gas-saturated rocks, and β is the constant defined from M, a, and b. In its limiting cases, the spheroid can represent a needle-like tubular pore ($a \to \infty$), a spherical pore ($a \to 1$), or thin "penny-shaped" crack ($a \to 0$). With the crack porosity known as a function of pressure (P) from compressibility measurements and using the value of $b = 0.008$, corresponding to air saturation, the Zimmerman model[15] yields the following expression for thermal conductivity:

$$\lambda = \lambda_0(T)\frac{[1-0.661\phi(P)]}{[1+41.3\phi(P)]} \tag{3}$$

$$\phi(P) = \phi_0 \exp(-P/P_0) \tag{4}$$

where $\phi(P)$ is the crack porosity at applied stress P, P_0 is the crossover pressure, ϕ_0 is the crack porosity at low pressures ($P = 0$), and $\lambda_0(T)$ is the thermal conductivity of solid at high pressures ($P \to \infty$) when all of the cracks are assumed to be closed. Equation 3 was used, as discussed below, to represent the present ETC data of rocks at high pressures.

Anand[47] studied the effects of a various physical properties on the ETC of dry sandstone samples. He used reported ETC data by Zierfuss and Viliet[49] to develop correlation equations for ETC. We have slightly modified the equation developed by Anand[47] by including one more fitting parameter (λ_2) as

$$\lambda = \lambda_0[1-\lambda_1\exp(-P/P_0)]^4 + \lambda_2 \tag{5}$$

where λ_i ($i = 0, 2$) are the fitting parameters. Equation 5 was used to represent the present experimental ETC data of rocks (see below).

The temperature dependence of the ETC for most crystalline rocks in the upper part of the crust at temperatures up to 600 °C can be expressed by the simple relation:[18]

$$\lambda^{-1} = A + BT/\mathrm{K} \text{ or } \lambda = \lambda_0/(1 + AT/\mathrm{K}) \tag{6}$$

This relation has been used by Seipold[29] to represent of the ETC results for granites and amphibolite. Buntebarth[1] determined A and B from measurements on 113 samples of metamorphic rocks in the temperature range from (50 to 200) °C. Kukkonen et al.[42] analyzed various correlation equations for the temperature and pressure dependence of the ETC of rocks. Several types of functions have been used by Seipold[39,40] and Clauser and Huenges[19] for the fitting of measured ETC data for rocks. The most common used functions is[103]

$$\lambda(T) = A + B/(350 + T/\mathrm{K}) \tag{7}$$

and eq 6. Equations 6 and 7 are valid at temperatures from (300 to 1300) K where phonon (lattice) conductivity dominates.

Hofmeister[90] studied the pressure and temperature dependences of the thermal conductivity of silicates from the Gruneisen parameter ($\gamma_{Th} = \alpha V K_T^2/C_V$), bulk modulus ($K_T$), and thermal expansivity (α):

$$\frac{d\ln\lambda}{dP} = \frac{1/3 + 4\gamma_{Th}}{K_T} \text{ or } \frac{d\ln\lambda}{dP} = \frac{1}{3K_T} + \frac{4\alpha V K_T}{C_V} \tag{8}$$

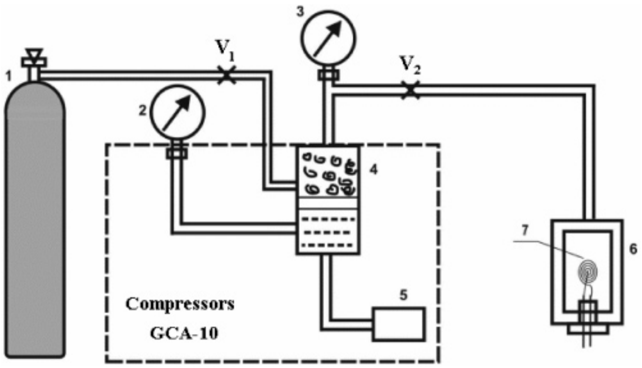

Figure 1. Experimental pressure measuring and pressure controlling unit: 1, gas cylinder; 2 and 3, standard manometers; 4, compressing cylinder; 5, compressor (GCA-10); 6, high-pressure chamber; 7, pressure transducer; V_1 and V_2, valves.

Discrepancies in d ln λ/dP reach 1000 % (see Hofmeister[75,90]) due to deformation, which alters the geometry of the samples, and cracking, which reduces thermal conductivity.[104−108] As one can see from eq 8, the second term of the pressure coefficient is d ln λ/d$P \approx K_T$. Therefore, at low pressures ($P < 100$ MPa), where K_T exhibits a sharp anomaly, the first term is small, while the second term is increasing proportionally to K_T. Therefore, d ln λ/dP at low pressures exhibits a rapid change. The dependence of the ETC of porous mica ceramic on porosity and compressibility (K_T) under pressure was discussed in our previous work.[28]

Seipold and Schilling[109] examined the ETC of a variety of serpentinities as a function of temperature at ambient pressure. The combined effects of pressure and temperature on the ETC are presented as $\lambda(P, T) = (1 + \alpha P)/(A + BT)$. The lattice thermal conductivity data derived from thermal diffusivity measurements were presented by Xu et al.[86] as

$$\lambda(P, T) = \lambda_{298}(298/T)^{1/2}(1 + \alpha P) \tag{9}$$

Experimental Apparatus and Procedure

The thermal conductivity apparatus and experimental procedure details were described in several of our previous publications.[24−28] The apparatus will only be briefly reviewed here. It consists of a high-pressure chamber, a thermal conductivity cell, an air thermostat, a high precision temperature regulator, and high-pressure liquid and gas compressors. In this method, thermal conductivity is obtained from simultaneous measurements of the steady-state heat flux and temperature gradient in the sample placed between the heating and cooling plates. Two thermocouples were embedded in the center of the inner surface of the bronze disk. The heater was located between these thermocouples. The other two thermocouples were soldered to the body of the heater. The temperature difference and temperature of the chamber were measured with four copper-constantan thermocouples. The pressure was created with liquid and gas compressors (Unipress Type GCA-10, Poland). The pressure in the chamber has been measured with a manganin pressure transducer with an uncertainty of 0.25 %. The pressure measuring and pressure controlling unit is schematic shown in Figure 1. Argon from the gas cylinder (1) under pressure (about 10 MPa) was supplied to the space above the piston of the cylinder (4). Then the valve V_1 was turned off and by using the compressor (5) (GCA-10), the oil was pumped to the space under the piston. The compressor (5) had two standard manometers (2 and 3). Manometer 2 read the pressure of the oil below the piston, while manometer 3 read the pressure of gas (argon) above the piston and in the high-pressure chamber (6). The readings of the both manometers were same. In the order to control the readings of the manometers (2 and 3), an additional manganin pressure transducer (7) was mounted in the high-pressure chamber (6). The difference between the readings of the manometers (2 and 3) and the pressure transducer (7) was almost zero.

The high-pressure chamber is located in the air thermostat. The temperature in the air thermostat was controlled automatically to within ± 5 mK. The thermal conductivity (λ) of the specimen was deduced from the relation

$$\lambda = \frac{Q - Q_{\mathrm{los}}}{\dfrac{S_1}{h_1}\Delta T_1 + \dfrac{S_2}{h_2}\Delta T_2} \tag{10}$$

where $Q = Q_1 + Q_2 + Q_{\mathrm{los}}$ is the heat flow transferred from the heater to the upper and lower specimens; $Q_1 = \lambda S_1/h_1\Delta T_1$ and $Q_2 = \lambda S_2/h_2\Delta T_2$ are the heat flows transferred by conduction through the lower and upper specimens, respectively; Q_{los} is the heat losses through the lateral surface of the samples; S_1 and S_2 are the cross-sectional areas of the specimens that heat flows through; h_1 and h_2 are the height of the samples; and ΔT_1 and ΔT_2 are the temperature differences across the samples thickness. The thermal conductivity was obtained from the measured quantities Q, Q_{los}, ΔT_1, ΔT_2, S_1, S_2, h_1, and h_2. The heat flow (Q) from the heater was distributed between the two samples (Q_1 and Q_2). The values of Q were corrected by a specimens side loss factor (Q_{los}). The values of Q_{los} were estimated from the relation

$$Q_{\mathrm{los}} = \lambda_{\mathrm{m}}\,\Delta T \frac{2\pi h}{\ln(d/D)} \tag{11}$$

where $d = 12$ mm and $D = 22$ mm are the diameter of the sample and the inner diameter of the high-pressure chamber, respectively; $h = h_1 + h_2$ is the height of the samples; λ_{m} is the thermal conductivity of the media of transmitted pressure (oil), and $\Delta T = T_{\mathrm{m}} - T_{\mathrm{C}}$ is the temperature difference between average values $T_{\mathrm{m}} = (T_2 + T_1)/2$ or $T_{\mathrm{m}} = (T_3 + T_4)/2$ of the temperatures (T_2 and T_3) of the lateral surface of the specimens and temperatures (T_1 and T_4) of the inner surface of the high-pressure chamber; $T_{\mathrm{C}} = T_1 = T_4$. The values of the temperature difference were almost constant, $\Delta T \approx 1.2$ K. The heat losses by conduction along the electrical leads, by radiation and heating, are negligibly small (see refs 26−28). The maximum relative uncertainty of thermal conductivity measurements associated with measured quantities can be estimated from the equation

$$\delta\lambda = \frac{\delta Q}{1 - \dfrac{Q_{\mathrm{los}}}{Q}} + \frac{\delta Q_{\mathrm{los}}}{\dfrac{Q_{\mathrm{los}}}{Q} - 1} + \frac{\delta S_1 + \delta h_1 + \delta(\Delta T_1)}{1 + \dfrac{S_2}{S_1}\dfrac{h_1}{h_2}\dfrac{\Delta T_2}{\Delta T_1}} + \frac{\delta S_2 + \delta h_2 + \delta(\Delta T_2)}{1 + \dfrac{S_1}{S_2}\dfrac{h_2}{h_1}\dfrac{\Delta T_1}{\Delta T_2}} \tag{12}$$

The uncertainties of all measured quantities are $\delta Q = 0.57$ %; $\delta Q_{\mathrm{los}} = 2$ %; $Q = 0.28$ W; $Q_{\mathrm{los}} = 0.02$ W; $\Delta T_1 = 2$ K; $\Delta T_2 = 1.5$ K; $\delta S_{1,2} = 0.33$ %; $\delta h_{1,2} = 0.33$ %; $\delta(\Delta T_{1,2}) = 0.1$ %. The propagation of uncertainties related to the uncertainties of pressure, temperature, and height are (0.03, 0.01, and 0.002) %, respectively. Heat losses through the side surface of the specimens were 3.5 % of the total amount of heat supplied to the specimens. Therefore, the total uncertainty in the thermal conductivity measurement stems from uncertainties in measured quantities of less than ± 2.0 %. To check the reproducibility, the measurements at each experimental temperature (T) and pressure (P) were repeated (5 to 10) times. The scatter of the experimental results did not exceed ± 0.5 %. The measurements were made with temperature differences ΔT_1 between (1 and 2) K.

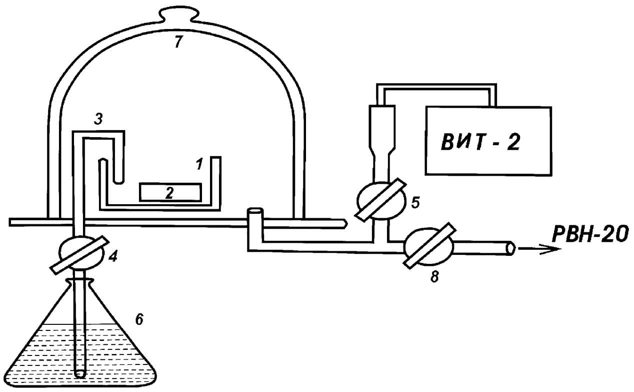

Figure 2. Experimental apparatus for the porosity measurements: 1, vessel; 2, speciment (rock); 3, feed tube; 4, 5, and 8, vacuum valves; 6, flask with pure water; 7, vacuum glass chamber; PBH-20, vacuum pump; BHT-2, electric vacuum-gauge.

In porous materials, heat is propagated basically by thermal conductivity through the solid, by radiation, and by convection through the pores. When the size of the pores are small ($r \approx 10^{-6}$ m, therefore a small temperature difference across the pores, $\Delta T_{\mathrm{pore}} \approx 0.003$ K), convection can be neglected. This makes it possible to minimize the risk of the convection in the pores. The absence of convection in the pores was verified experimentally by measuring the thermal conductivity with various temperature differences ΔT_1. Heat transfer by radiation increases as the pore size is increased, and its effect can be calculated by the method described in our previous publications.[26−28] Because it has a T^3 ($\lambda^{\mathrm{rad}} = 4f\epsilon\sigma T^3 r$) dependence, variation obviously plays an increasingly active role at high temperatures (≈1200 K). In this work it has been assumed that the solid phase is transparent to thermal radiation. Therefore, heat transfer through the pores by radiation can be neglected.

Cylindrical rock samples 12 mm in diameter and 3 mm in length were prepared from cored samples of the original rock blocks. Before measurements, the samples were dried at a temperature of 120 °C for (5 to 6) h and then were slowly cooled. Then the porosity of the specimens was measured by using the apparatus shown in Figure 2. To determine the porosity, the samples were saturated with pure water under vacuum. Vacuum pump PBH-20 was used to evacuate air from the glass chamber (7). After reaching a vacuum 5×10^{-2} in the chamber (7), the vacuum-gauge (BHT-2) was isolated by using the valve (5). Then the vessel (1) was filled with pure water by using valve 4 at room temperature (20 °C). The specimen was saturated with pure water for 72 h. The specimen was weighted before (dry) and after saturation. Porosity (ϕ) was calculated from the ratio pore volume (V_{P}) to the total volume of the dry rock (V_{rock}):

$$\phi/(\%) = 100(V_{\mathrm{P}}/V_{\mathrm{rock}}) \quad \text{with } V_{\mathrm{P}} = (m_{\mathrm{sat}} - m_{\mathrm{dry}})/\rho_{\mathrm{w}} \text{ and } V_{\mathrm{rock}} = m_{\mathrm{dry}}/\rho_{\mathrm{dry}} \tag{13}$$

where V_{P} is the volume of the pores; V_{rock} is the volume of dry rock; m_{sat} and m_{dry} are the mass of saturated and dry rock, respectively; ρ_{w} and ρ_{dry} are the density of water and dry rock at atmospheric pressure and at room temperature. The uncer-

Table 1. Experimental Effective Thermal Conductivities of Rocks as a Function of Temperature and Pressure

Sandstone (Aktash, Dagestan, Russia, 2977 m, Porosity of $m = 5$ %)

	$\lambda/(\mathrm{W \cdot m^{-1} \cdot K^{-1}})$ at P/MPa					
T/K	0.1	50	100	150	200	250
273	2.01	2.05	2.08	2.10	2.12	2.14
323	1.93	1.96	1.99	2.01	2.03	2.05
373	1.88	1.91	1.93	1.94	1.96	1.98
423	1.82	1.85	1.87	1.88	1.90	1.92

Limestone (Soltagasha, Dagestan, Russia, 201 m, Porosity of $m = 5$ %)

	$\lambda/(\mathrm{W \cdot m^{-1} \cdot K^{-1}})$ at P/MPa					
T/K	0.1	50	100	150	200	250
273	1.94	2.13	2.19	2.21	2.22	2.25
323	1.78	2.01	2.06	2.07	2.08	2.10
373	1.65	1.91	1.94	1.96	1.97	1.98
423	1.55	1.84	1.86	1.87	1.88	1.89

Amphibolite (Kola Ultra-Deep Borehole Sample, 10000 m, Porosity of $m = 1$ %)

	$\lambda/(\mathrm{W \cdot m^{-1} \cdot K^{-1}})$ at P/MPa							
T/K	0.1	50	100	150	200	250	300	350
275	3.52	3.78	3.87	3.91	3.93	3.95	3.97	3.99
323	3.02	3.27	3.35	3.40	3.42	3.44	3.46	3.48
373	2.63	2.89	2.98	3.06	3.08	3.10	3.12	3.14
423	2.35	2.58	2.70	2.75	2.78	2.81	2.83	2.85

Granulite (Saxonian Granulite Mountains, Germany, Porosity of $m = 1$ %)

	$\lambda/(\mathrm{W \cdot m^{-1} \cdot K^{-1}})$ at P/MPa						
T/K	0.1	25	50	100	150	200	250
273	2.06	2.14	2.19	2.27	2.31	2.34	2.37
323	1.96	2.06	2.13	2.19	2.24	2.28	2.31
373	1.85	1.97	2.06	2.11	2.16	2.20	2.23
423	1.77	1.87	1.93	2.04	2.09	2.13	2.15

Pyroxene−Granulite (Saxonian Granulite Mountains, Germany, Porosity of $m = 1.2$ %)

	$\lambda/(\mathrm{W \cdot m^{-1} \cdot K^{-1}})$ at P/MPa						
T/K	0.1	25	50	100	150	200	250
273	2.06	2.14	2.19	2.27	2.31	2.34	2.37
323	1.96	2.06	2.13	2.19	2.24	2.28	2.31
373	1.85	1.97	2.06	2.11	2.16	2.20	2.23
423	1.77	1.87	1.93	2.04	2.09	2.13	2.15

tainty of the porosity determination from this method was about 0.4 %. Only the open and interconnected pore space can be evaluated by this method.

To check and confirm the validity of the method and procedure of the measurements, the thermal conductivity measurements were made with standard (reference) materials (fused quartz and quartz ceramic) in our previous study[27] using the present apparatus. Excellent agreement within ± 0.5 % was found between our value and literature data. This excellent agreement for fused quartz and quartz ceramic demonstrates the reliability and accuracy of the present measurements for rocks and correct operation of the instrument.

Characteristics of the Samples

The samples contained open and interconnected pores with random orientation. The brief description of physical and chemical characteristics of the samples is given below.

Sandstone. The density was 2.18 $\mathrm{g \cdot cm^{-3}}$, weakly cemented, weakly carbonated, color is gray, moderate grained, and porosity was 5 %. The sample come from Aktash, Dagestan, Russia, borehole #1, depth 2977 m (80 to 90) %. The forming material basically has crystalline structure.

Limestone. The density was 2.38 $\mathrm{g \cdot cm^{-3}}$, porosity was 5 %. Origin of the sample was the Soltagasha, Dagestan, Russia, borehole #96, depth 201 m. The forming material had a crystalline structure.

Amphibolite. The density was 2.61 $\mathrm{g \cdot cm^{-3}}$; porosity was 1 %. The sample was taken for the study in the Kola ultra-deep borehole; strong (hard) packing structure. The forming material had a crystalline structure. The sample was collected from wells in a depth interval of 10000 m.

Granulite. Quartz 38 %, plagioclase 9 %, K-feldspar 47 %, biotite 1 %, and granite 4 %; sampled at the location Saxonian Granulite Mountains, Germany. The structure was fine grained. Porosity was 1.0 %. The density was 2.06 $\mathrm{g \cdot cm^{-3}}$. The forming material was a mix of the crystalline and amorphous structure.

Pyroxene−Granulite. Clinopyroxene 39 %, plagioclase 34 %, opaque minerals 11 %, orthopyroxene 9 %, granite 6 %, ambibol <1 %. The structure was fine grained. The grains were not oriented and almost the same size (plagioclase, 0.15 mm and granite (0.5 to 0.8) mm). Porosity was 1.2 %. The density was 3.27 $\mathrm{g \cdot cm^{-3}}$, mostly amorphous structure; sampled at the location Saxonian Granulite Mountains, Germany.

Results and Discussions

The results of ETC measurements for five dry rocks (sandstone, limestone, amphibolite, granulite, and pyroxene−granulite) with porosities between (1 and 5) % are reported in Table 1. Temperature dependence was measured from (273 to 423) K at 50 K intervals, and pressure dependence up to 350 MPa at 50 MPa intervals. Figures 3 and 4 show the experimental

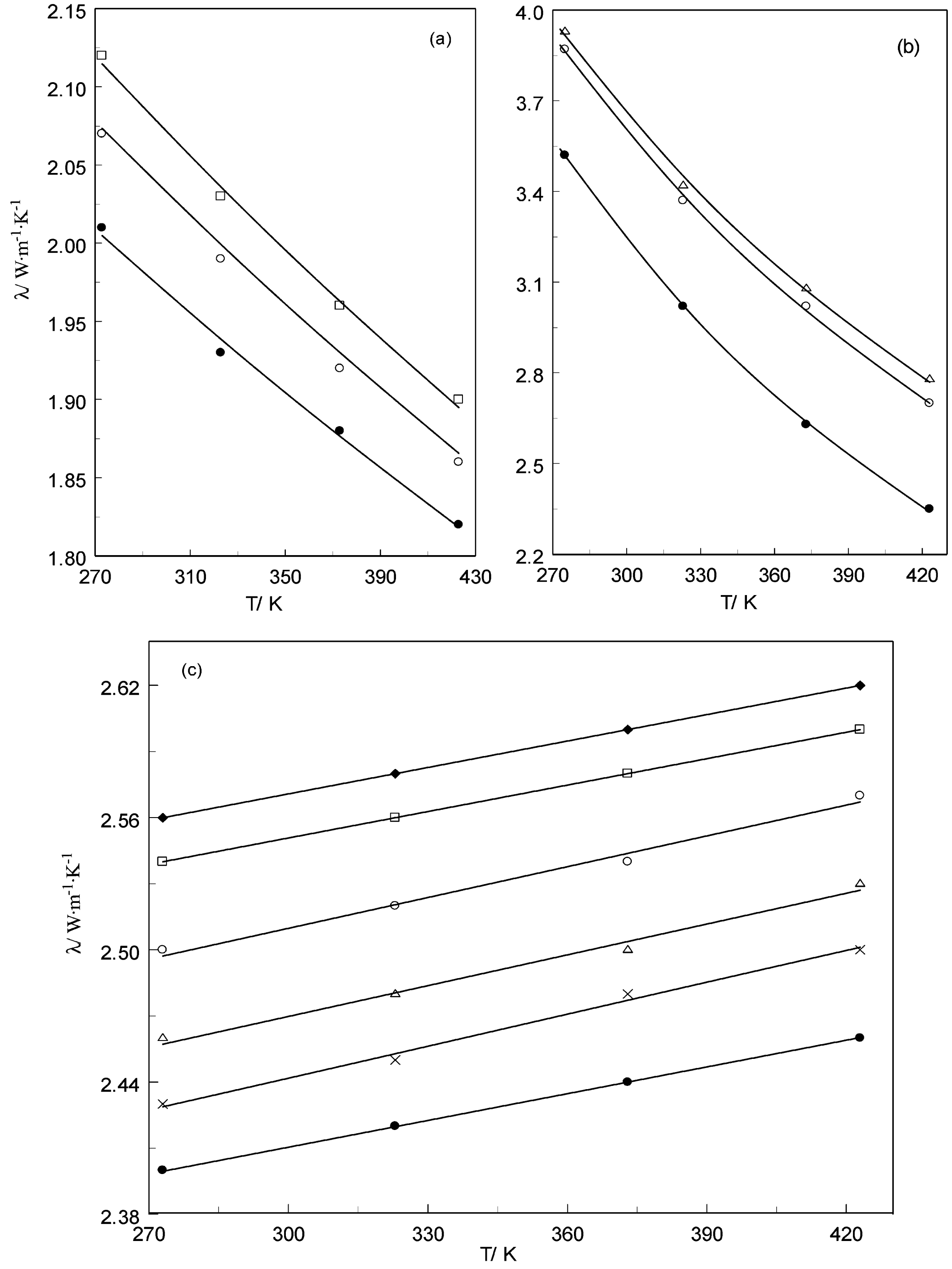

Figure 3. Experimental ETC of rocks as a function of temperature along various isobars together with values calculated with eqs 6 and 14. (a) Sandstone ($m = 5$ %). (b) Amphibolite ($m = 1$ %). (c) Pyroxine−granulite (1.2 %). ●, 0.1 MPa; △, 50 MPa; ○, 100 MPa; ×, 150 MPa; □, 200 MPa; ♦, 250 MPa; ■, 300 MPa.

ETC of the rocks as a function of pressure and temperature, respectively. Equation 9 predicts the present ETC data to within (10 to 15) % at high temperatures and (5 to 6) % at low temperatures.

Effect of Pressure on the Thermal Conductivity of Rocks. Effect of pressure on ETC is smaller than the effect of temperature. The pressure effect on ETC strongly depends on the rocks nature, from mineralogical composition, porosity, and density. The ETC of rocks increases with pressure. However, the effect of pressure on ETC of porous materials is different for distinct pressure range. The fractures and microcracks developed after stress release, when the sample was brought to the surface, begin to quickly close (some pores closing completely and others become narrow) again with increasing pressure leading to a decrease in internal thermal resistances of the sample (increasing mechanical contacts between the grains[121]). This reduces thermal contact resistance as well as porosity and density. At a cross-over pressure {between (50 to 100) MPa depending on initial porosity of the rock} this process comes to an end. Therefore, a rapid increase of the ETC was noted at low pressures (below 100 MPa) (see Figure 4). Some authors have missed this low pressure range where the rapid pressure dependence of the ETC of porous materials is observing. At high pressures when all of the cracks are assumed to be closed, a further pressure increase does not affect thermal conductivity significantly (see Figure 4). If the pressure continues to increase, there is reduction of the rock’s intrinsic porosity that is not artificially created by stress release. The same behavior of the

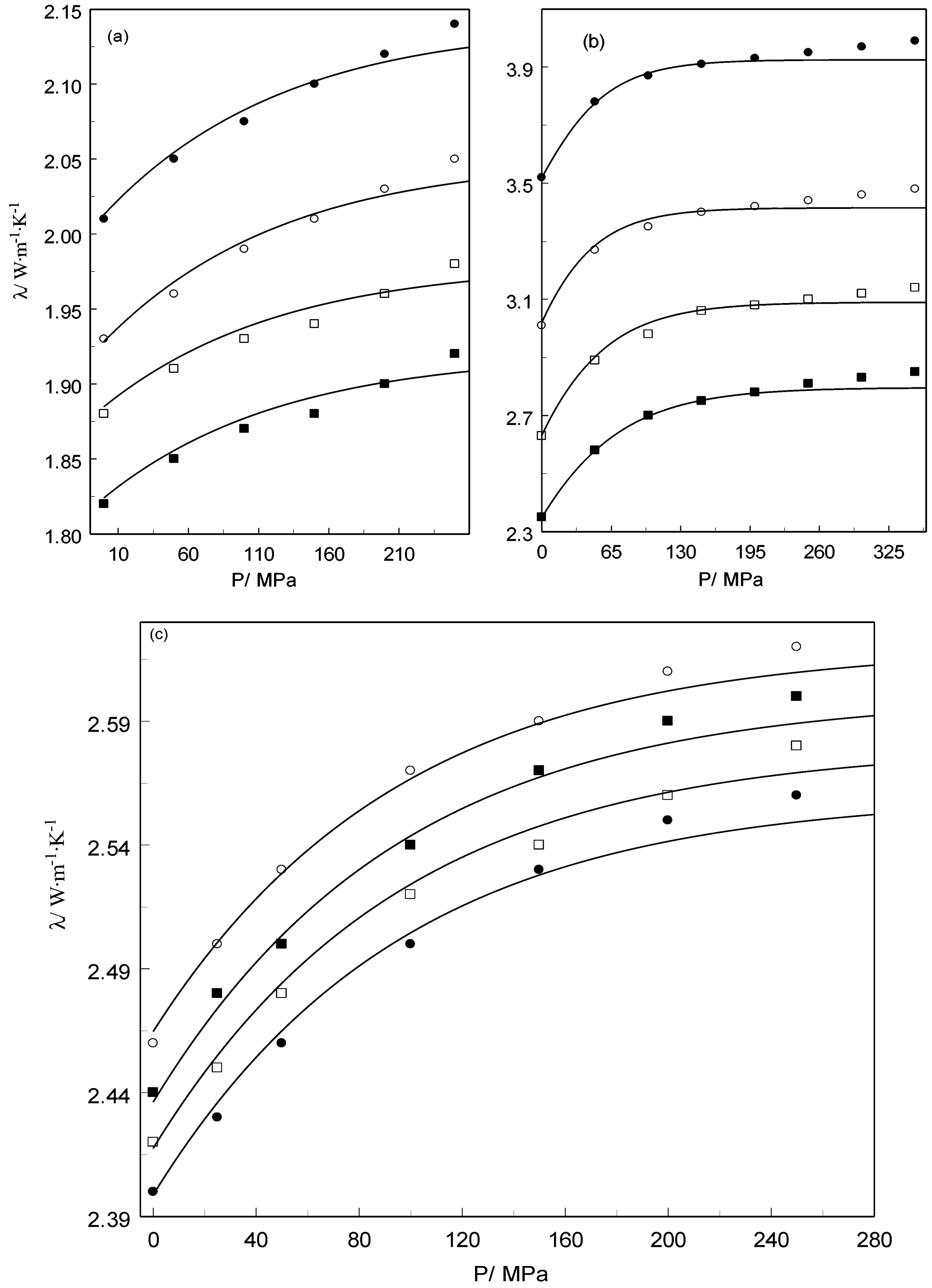

Figure 4. Experimental ETC of rocks as a function of confining pressure along various isotherms together with values calculated with eq 3. (a) Sandstone (m = 5 %). (b) Amphibolite (m = 1 %). (c) Pyroxine−granulite (1.2 %). ●, 273 K; ○, 323 K; □, 373 K; ■, 423 K; —, eq 3.

ETC in the low-pressure range was found for most rocks (see, for example, refs 19−23, 33, 42, 43, and 110). For some rocks the increasing of the ETC at pressures up to 50 MPa was reached up to 100 % (see, for example, ref 21). The linear behavior of pressure dependence of the ETC of rocks at high pressures is typical as reported by many other authors.[19,42,43,69,76,77,109,111] For rocks with small porosity, the increase of the ETC is about 1.3 % per 10 MPa.[20,22,23] Edmondson[50] has found the increases in ETC of sandstones to be (8 to 12) % per 7 MPa in the stress range of (6 to 25) MPa. Woodside and Messmer[70,71] reported almost the same results of 11.5 % per 7 MPa in the stress range of between (0 and 7) MPa and 2.5 % per 7 MPa in the range of from (14 to 28) MPa. The present ETC increases by about (0.1 to 0.27) % per 10 MPa in the high-pressure range. The measured ETC were used to calculate the pressure coefficient ($d\ln\lambda/dP$) for each rock. The derived values of $d\ln\lambda/dP$ are given in Table 2. This table does not include the values of $d\ln\lambda/dP$ at pressures below 100 MPa where rapid changes in ETC are observed. As one can see from Table 2, the pressure coefficient of ETC for rocks under study is changes within (0.076 to 0.81) GPa^{-1}. The pressure dependence of the ETC of rocks reported by some authors [Kukkonen et al.,[42] Osako et al.,[76] and Kutsura[111] (for thermal diffusivity)] is very small (0.03 to 0.04) GPa^{-1}. Horai and Susaki[43] found that in the pressure range from (2 to 12) kbar the rate of pressure change of the ETC ($d\lambda/dP$) of rocks is >0.09 $W\cdot m^{-1}\cdot K^{-1}\cdot kbar^{-1}$. The highest rate of 0.33

Table 2. Values of the Pressure Coefficient of Rocks as a Function of Temperature

	$(\mathrm{d}\ln\lambda/dP)/10^{-3}$ MPa^{-1}				
***T*/K**	sandstone	limestone	amphibolite	granulite	pyroxene−granulite
273	(0.076−0.08)	(0.15−0.16)	(0.10−0.11)	(0.56−0.61)	(0.36−0.38)
323	(0.19−0.20)	(0.12−0.13)	(0.11−0.12)	(0.72−0.81)	(0.36−0.38)
373	(0.17−0.18)	(0.13−0.14)	(0.12−0.13)	(0.72−0.81)	(0.36−0.38)
423	(0.17−0.18)	(0.10−0.11)	(0.17−0.18)	(0.62−0.62)	(0.31−0.33)

W·m^{-1}·K^{-1}·kbar^{-1} was found for crystalline quartz. The values of pressure coefficient for amphibolites and granites reported by Seipold[30] are (0.08 to 0.25) GPa^{-1} are close to our results of (0.1 to 0.18) GPa^{-1} (see Table 2). The data reported by Seipold et al.[39] shows the values of pressure coefficients are (0.016 to 0.16) GPa^{-1}. Measurements of olivine by Beck et al.[69] show a pressure dependence in λ of (5 to 6) GPa^{-1}. The pressure dependence of thermal diffusivity for forsterite reported by Fujisawa et al.[112] shows a higher value than reported by other authors. The calculation by Hofmeister[89] shows the values of d ln λ/dP for some minerals vary within (0.021 to 0.28) GPa^{-1}. Ljubimova et al.[113] reported that the values of pressure coefficient for some rocks are within (0.02 to 0.70) GPa^{-1}. Therefore, the literature values of the pressure coefficient of ETC for various rock types cover a wide range depending on the nature of rocks and their mineralogical and structural characteristics. Most thermophysical, electrical, and acoustical properties of porous materials show typical pressure dependence.[33,46,114−120]

The cross-over pressure results from a sharp changing in volume compressibility, $K_T = 1/V(\partial V/\partial P)_T$, of rocks with pressure increasing.[46,119,122] Brace[119] shows that in the pressure range up to 50 MPa, very high volume compressibility was found due to the closure of great airfilled cracks. At pressures higher than 50 MPa a smaller constant compressibility was reached. Similar results were observed by Wang et al.[57] for granite samples after thermal stress cracking. The compressibility K_T above 100 MPa varies slightly from linear behavior with pressure.[46,114−118] At pressures about 400 MPa the porosity of the samples changed (exponentially, see eq 4) is about (1 to 2) %. As porosity decreased the convective conductivity in the pore space is also decreased. The ETC decreased considerably with increased porosity [$\lambda = \lambda_0(1 - \phi)$,[4] see, for example, refs 47 and 21]. Therefore, the ETC of porous materials is changing due to porosity change is about (0.04 to 0.07) W·m^{-1}·K^{-1}.[27,28]

To describe of the pressure dependence of ETC of rocks we have slightly modified the Zimmerman's model[15] by including one more parameter, namely, the cross-over pressure P_0 and $\lambda_0(T)$ as a function of temperature (see eq 3). This is physically very clear because cross-over pressure (P_0) strongly depend on the rocks characteristics and varies from (10 to 150) MPa. The measured ETC data for rocks samples were fitted to the eq 3. Figure 4 shows the comparison of the calculated with eq 3 and experimental values of ETC of rocks. The agreement between the present experimental data and calculated values of ETC is excellent (average absolute deviation, AAD, between (0.13 and 0.56) % over the entire range of pressure). The values of the cross-over pressure (P_0) and reference porosity parameter (ϕ_0) together with values of λ_0 as a function of temperature derived with present ETC data are given in Table 3. As one can see from Table 3, the value of P_0 is almost constant for most rocks. The values of ϕ_0 are slightly changes with temperature due to thermal expansion. Figure 5 demonstrates the effect of parameter ϕ_0 on the pressure dependency of ETC. As Figure 5 shows, the low pressure anomaly of the ETC strongly depends on the values of ϕ_0. Equation 5 was also used to represent the present ETC data as a function of T and P. The fitted results are given in Table 4. Figure 6 shows comparisons of the pressure dependences of the present ETC measurements for various type rocks at a selected temperature (323 K). This figure demonstrates the effect of the nature of the rocks on the values and pressure dependence of the ETC of rocks. As one can see from Figure 6, the amphibolite shows the highest values of ETC among the other rocks at the same thermodynamic (P and T) conditions, while sandstone observed lowest values.

Table 3. Values of the Parameters P_0 and ϕ_0 in Equations 3 and 4 as a Function of Temperature for Various Types of Rocks

***T*/K**	P_0/MPa	ϕ_0	λ_0/W·m^{-1}·K^{-1}
	Sandstone		
273	120	0.0015	2.14
323	120	0.0015	2.05
373	120	0.0012	1.98
423	120	0.0012	1.92
	Limestone		
273	50	0.0450	2.25
323	35	0.0450	2.10
373	30	0.0500	1.98
423	30	0.0500	1.89
	Amphibolite		
273	125	0.0028	4.52
323	138	0.0040	3.98
373	150	0.0051	3.59
423	150	0.0063	3.26
	Granulite		
273	70	0.0038	2.37
323	70	0.0045	2.31
373	70	0.0052	2.23
423	70	0.0055	2.15
	Pyroxene−Granulite		
273	90	0.0016	2.56
323	90	0.0016	2.58
373	90	0.0016	2.60
423	90	0.0015	2.62

Effect of Temperature on the Thermal Conductivity of Rocks. The temperature dependence of ETC depends also on rock-type. Lattice or phonon thermal conductivity varies inversely with temperature ($\lambda \approx T^{-1}$). The thermal expansivity

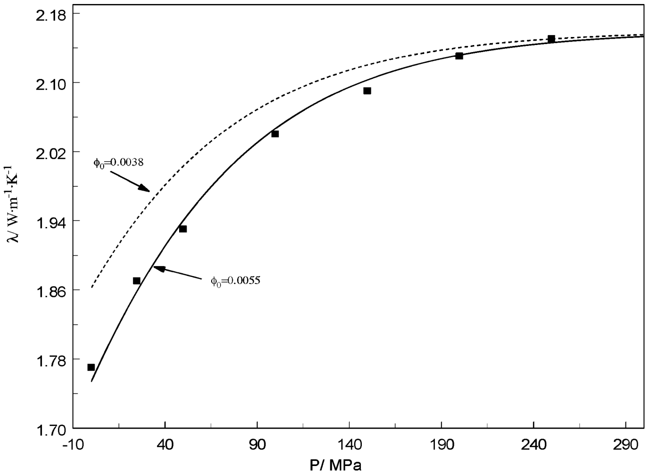

Figure 5. Effects of parameter (ϕ_0) on pressure dependence of the ETC of granulite (m = 1 %) at temperature 423 K: −, eq 3.

Table 4. Values of the Parameters λ_i ($i = 0, 2$) and P_0 in Equation 5 as a Function of Temperature for Various Type of Rocks

T/K	λ_0/W·m^{-1}·K^{-1}	λ_1	λ_2/W·m^{-1}·K^{-1}	P_0/MPa
		Sandstone		
273	0.2085	0.3797	1.9791	140
323	0.1957	0.3356	1.8923	140
373	0.1511	0.5244	1.8734	140
423	0.1511	0.5244	1.8134	140
		Limestone		
273	1.9540	0.0392	0.2821	60
323	1.2334	0.0669	0.8497	40
373	0.7518	0.1283	1.2172	30
423	0.3903	0.3635	1.4872	20
		Amphibolite		
273	0.6266	0.2296	3.2990	40
323	0.9548	0.1249	2.4607	40
373	1.2279	0.1103	1.8626	50
423	1.0717	0.1265	1.7255	60
		Granulite		
273	0.3979	0.2925	1.9680	70
323	0.2098	0.0404	0.1996	70
373	0.7585	0.1530	1.4679	70
423	0.5430	0.2656	1.6184	70
		Pyroxene−Granulite		
273	0.3355	0.1745	2.2439	100
323	0.3322	0.1664	2.2601	100
373	0.3661	0.1496	2.2511	100
423	0.9017	0.0515	1.7330	100

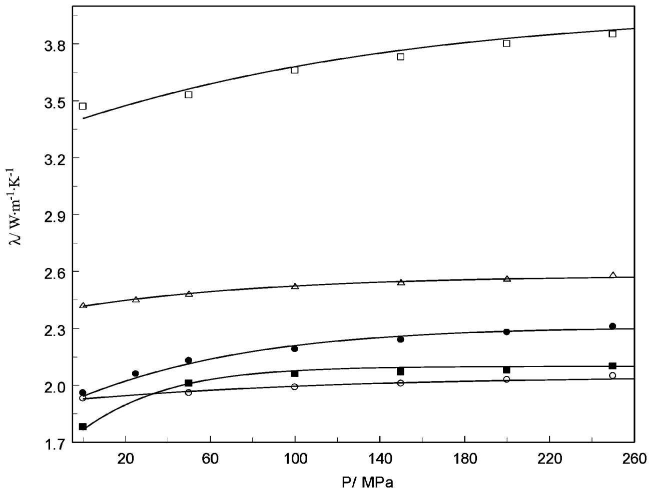

Figure 6. Comparison of experimental pressure dependence of the thermal conductivity for various type rocks at selected temperature of 323 K: ●, granulite (1 %); △, pyroxine−granulite (1.2 %); ○, sandstone (m = 5 %); □, amphibolite (m = 1 %); ■, limestone (m = 5 %); −, eq 3.

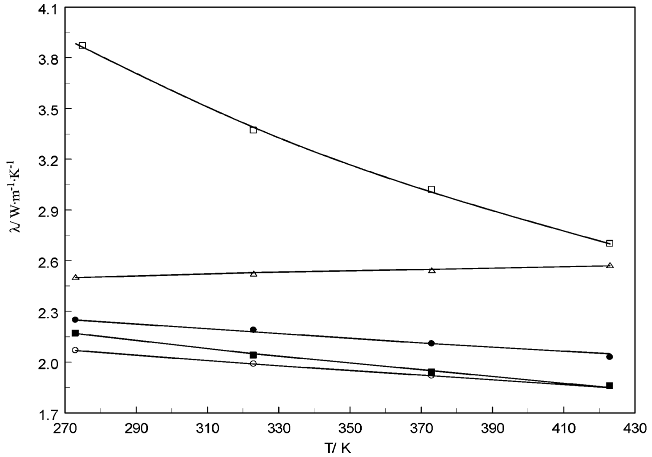

Figure 7. Comparison of experimental temperature dependence of the ETC for various type rocks at selected pressure of 100 MPa: ●, granulite (1 %); △, pyroxine−granulite (1.2 %); ○, sandstone (m = 5 %); □, amphibolite (m = 1 %); ■, limestone (m = 5 %); −, eqs 6 and 14.

increases with temperature and cracking may create contact resistances between mineral grains, thus contributing to the observed decrease of ETC with temperature. Closed cracks act as scattering centers for the heat carrying phonons[39,40] (interrupting of the crystal lattice scatters the phonons). For most of the rocks with crystalline structure the ETC decreases monotonically with increase in temperature[123] until around (700 to 1200) °C. Radiation of heat is efficient only at high temperatures {≈ (700 to 1200) °C}. Therefore, radiative thermal conductivity will not be treated here. A review of heat radiation in the Earth is given by Clauser.[124] The radiative thermal conductivity, in contrast, increase with temperature as $\lambda \approx T^3$. Thus the ETC of rocks as a function of temperature shows initially a decrease with T, until (700 to 1200) °C where the radiative component inverts this decreasing trend. For polycrystalline rocks the ETC decrease is about (1 to 5) % per 10 K. The experimental ETC of the rock studied as a function of temperature along selected isobars is shown in Figure 3. The comparison of the temperature dependencies of the ETC of various rocks types is shown in Figure 7. The values of temperature coefficient ($d\ln\lambda/dT$) of the ETC for sandstone, limestone, amphibolite, and granulite derived from the present experimental data are given in Table 5. Heterogeneity provides a dramatic change in the temperature dependence of ETC thorough compositional effects. The ETC of rocks depends on the conductivity of its mineral components, the conductivity of pore fluids, the extent and geometry of the pore space, and the orientation of the pores. Rocks are very complicated and consist of oxides and minerals with various chemical elements. Therefore, the temperature dependences of the ETC of rocks strongly depend on the conductivity of its skeleton solid mineral components (rock-forming minerals and cementation substance) from which it is formed. For example, the decrease of ETC with T is quite different, depending on the feldspar content. Rocks with high feldspar content show an increase in ETC with temperature of some plagioclase feldspars which compensate the decrease in ETC with increase in temperature observed for other minerals and rocks. The rocks that are rich in feldspar show a decrease in ETC with T about 10 %, while for rocks that are poor in feldspar decrease more than 40 %.[19] The ETC of some rocks with high feldspar content is relative independent of temperature or even increase with temperature.[18] The pyroxene−granulite, which contains 34 % plagioclase, shows an increase of the ETC with T (see Figure 3c). The ETC of rocks decrease with temperature as porosity and amorphous phase in rocks increase. The ETC of crystalline rocks decreases almost linearly at temperatures up to (700 to 1200) °C (see Figure 3a,b). Thermal conductivity of rocks with a high amorphous phase (for example, volcanic or magnetite containing rocks) linearly increases with temperature. For amorphous materials (for example, fused quartz, silica glasses, and vitreous materials) the thermal conductivity increases with temperature as[127] $\lambda \propto T^n$, where $n > 0$. The increase of the thermal conductivity of fused quartz with temperature was studied by refs 27, 43, and 128. Therefore, temperature dependence of the ETC in rocks materials depends whether crystalline or amorphous structure dominate. More complicated behavior of the ETC is found for rocks with mixture of amorphous and crystalline structure. The thermal conductivity for mixed crystals varies more slowly than $\lambda \propto T^{-n}$, where $0 < n < 1$. Pyroxene−granulite is a mixed crystalline and amorphous structure. Since the ETC for pyroxene−granulite increase with temperature, therefore, in this sample the amorphous structure dominates crystalline components. Therefore, precise thermal

Table 5. Values of the Temperature Coefficient of Rocks as a Function of Pressure

	$(\mathrm{dln}\lambda/\mathrm{d}T)/10^{-4}\ \mathrm{K}^{-1}$				
P/MPa	sandstone	limestone	amphibolite	granulite	pyroxene−granulite
0.1	(6.2−6.8)	(14−17)	(23−34)	(9−11)	(1.6−1.7)
50	(6.4−7.1)	(9−11)	(21−31)	(8−9)	(1.8−1.9)
100	(6.7−7.4)	(10−12)	(20−29)	(7−8)	(1.8−1.9)
150	(7.0−7.8)	(10−12)	(20−29)	(6−7)	(1.6−1.7)
200	(6.9−7.7)	(10−12)	(19−28)	(6−7)	(1.6−1.7)
250	(7.0−7.7)	(11−13)	(19−28)	(6−7)	(1.5−1.6)

Table 6. Values of Parameter λ_0 and A in Equations 6 and 14 as a Function of Pressure for Various Types of Rocks

	P/MPa					
	0.1	50	100	150	200	250
			Sandstone			
$\lambda_0/\mathrm{W{\cdot}m^{-1}{\cdot}K^{-1}}$	2.465	2.531	2.601	2.664	2.681	2.669
$A \times 10^4/\mathrm{K^{-1}}$	8.406	8.766	9.318	9.940	9.807	9.677
			Limestone			
$\lambda_0/\mathrm{W{\cdot}m^{-1}{\cdot}K^{-1}}$	3.602	2.996	3.259	3.304	3.311	3.455
$A \times 10^4/\mathrm{K^{-1}}$	3.152	1.505	1.797	1.828	1.814	1.979
			Amphibolite			
$\lambda_0/\mathrm{W{\cdot}m^{-1}{\cdot}K^{-1}}$	52.824	26.218	19.216	17.752	16.897	16.140
$A \times 10^4/\mathrm{K^{-1}}$	5.099	2.157	1.446	1.293	1.206	1.129
			Granulite			
$\lambda_0/\mathrm{W{\cdot}m^{-1}{\cdot}K^{-1}}$	2.983	2.898	2.874	2.879	2.877	2.936
$A \times 10^4/\mathrm{K^{-1}}$	1.627	1.142	0.9685	0.8912	0.8249	0.8548
			Pyroxene−Granulite			
$\lambda_0/\mathrm{W{\cdot}m^{-1}{\cdot}K^{-1}}$	2.289	2.330	2.370	2.409	2.429	2.449
$A \times 10^4/\mathrm{K^{-1}}$	4.048	4.659	4.659	4.257	4.257	4.048

conductivity measurements can provide information about the order of crystallization of the rocks. Horai and Susaki[43] found that for andesite the ETC is far less temperature dependence.

Eucken[125] found that thermal conductivity of crystalline materials decreases with temperature according to the eq 6. The values of λ_0 and A for some porous materials have been calculated.[18,19,42,126] The present ETC results for sandstone, limestone, amphibolite, and granulite were fitted to eq 6, while for the pyroxene−granulite we used the linear relation

$$\lambda = \lambda_0 + AT \qquad (14)$$

The values of fitting parameters λ_0 and A are given in Table 6.

The temperature and pressure are not the only sources that define the ETC behavior of rocks.[129] The temperature dependence of ETC of rocks strongly depend also on the quartz content. High content of quartz results in a high value of conductivity and a rapid decrease of λ with increasing temperature. Rocks having a low content of quartz exhibit a much smaller temperature dependence of λ. Ozbek[94] considered the various methods of estimating solids thermal conductivity for a mineral assemblage. Quartz, having the highest conductivity of common rock-forming minerals, dominates thermal behavior of the assemblage. The ETC for higher quartz content solid materials can be estimated by the following equation[94] $\lambda = 7.7Q + 2.85(1 - Q)$, where Q is the fraction quartz content. The technique of determination of the ETC of rocks from the mineralogical composition was developed in the works.[59,60,130] Pribnow and Umsonst[59,60] developed a layered model to predict the thermal conductivity of rocks from the mineral content. The estimated values of the thermal conductivity are strongly controlled by the quartz, amorphous, and/or crystalline content.

Conclusion

By means of the steady-state parallel plate apparatus the λ, P, T relationships for five dry rocks (sandstone, limestone, amphibolite, granulite, and pyroxene−granulite) with porosities between (1 and 5) % were measured in the temperature range (273 to 423) K and at pressures up to 350 MPa with an estimated uncertainty of ± 2.0 %. The effect of pressure and temperature on the ETC behavior of rocks was studied. A sharp increase of the ETC was found for rocks at low pressures (between 0.1 and 100 MPa). At high pressures ($P > 100$ MPa) a weak linear dependence of the ETC with pressure was observed. The pressure and thermal coefficients were derived using the measured ETC as a function of temperature and pressure. The measured values of ETC of rocks were used to test and confirm of applicability of various theoretical and semiempirical models. The effect of the structure (size, shape, and distribution of the pores) and mineralogical compositions on ETC of various rocks types was studied. Reported in this work are the values of ETC for rocks that can be used to test and improve the existing theoretical models which can be applied to estimate thermal conductivities of all types of rocks at high temperatures and high pressures. The observed character of the temperature dependence of ETC of pyroxene−granulite confirmed that its structure is mostly amorphous, while for other rocks (sandstone, limestone, amphibolite, and granulite) the structure is basically crystalline.

Acknowledgment

I.M.A. thanks the Physical and Chemical Properties Division at the National Institute of Standards and Technology (NIST) for the opportunity to work as a Guest Researcher at NIST during the course of this research. The authors would also like to thank Dr. U. Seipold for providing the rock samples (Granuliteand Pyroxene-Granulite from Saxonian Granulite Mountains, Germany).

Literature Cited

(1) Buntebarth, G. The thermal properties of KTB Oberpfalz VB core sample at elevated temperature and pressure. *Sci. Drill.* **1991**, *2*, 73−80.

(2) Huenges, E.; Burkhard, H.; Erbas, K. Thermal conductivity profile of the KTB pilot corehole. *Sci. Drill.* **1990**, *1*, 224−230.

(3) Dubuffet, F.; Yuen, D. A.; Rabinowicz, M. Effects of a realistic mantle thermal conductivity on the patterns of 3-D convection. *Earth Planet. Sci. Lett.* **1999**, *171*, 401−409.

(4) Clauser, C.; Villinger, H. Analysis of conductive and convective heat transfer in a sedimentary basin, demonstrated for the Rheingraben. *Geophys. J. Int.* **1990**, *100*, 393−414.

(5) Čermak, V. Lithosphere thermal regimes in Europe. *Phys. Earth Planet. Int.* **1993**, *79*, 179−193.

(6) Williams, C. F.; Sass, J. H. The role of temperature-dependent thermal conductivity in heat transfer at the geysers. *Procedings of the International Association of Seismology and Physics of the Earth's Interior*, 27th General Assembly, Wellington: New Zealand, 1994.

(7) Luchenbruch, A. H.; Sass, J. H. Heat flow in the United States. In *The Earth's Crust*; Heacock, J. G., Ed.; AGU: Washington, DC, 1977; pp 626−675.

(8) Pribnow, D.; Williams, C. F.; Sass, J. H.; Keating, R. Thermal conductivity of water-saturated rocks from KTB pilot hole at temperatures of 25 to 300 °C. *Geophys. Res. Lett.* **1996**, *23*, 391−394.

(9) Sass, J. H.; Lachenbruch, A.; Munroe, R.; Greene, G.; Moses, T. Heat flow in the western United States. *J. Geophys. Res.* **1971**, *76*, 6376−6413.

(10) Sass, J. H.; Lachenbruch, A.; Munroe, R. Thermal conductivity of rocks from measurements on fragments and its application to heat-flow determinations. *J. Geophys. Res.* **1971**, *76*, 3391−3401.

(11) Buntebarth, G. *Geothermics*; Springer: Berlin, 1984.

(12) Somerton, W. H. Some characteristics of porous rocks. *J. Pet. Technol.* **1958**, *213*, 61−64.

(13) Somerton, W. H.; Keese, J. A.; Chu, S. C. Thermal behavior of unconsolidated oil sands. *SPE J.* **1974**, *14*, 513−521.

(14) Boberg, T. C. *Thermal Methods of Oil Recovery*; John Wiley: Somerset, NJ, 1988.

(15) Zimmerman, R. Thermal conductivity of fluid saturated rocks. *J. Pet. Sci. Eng.* **1989**, *3*, 219−227.

(16) Kaviany, M. *Principles of Heat Transfer in Porous Media*, 2nd ed.; Springer: New York, 1991.

(17) Robertson, E. C. *Physical Properties of Limestone and Dolomite Cores from the Sandhill Well, Wood County, West Verginia*; Report of Investigations 18; West Verginia Geological Servey: Morgantown; pp 112−144.

(18) Čermak, V.; Rybach, L. Thermal conductivity and specific heat of minerals and rocks. In *Landolt and Börnstein V/1: Physical Properties of Rocks*; Angenheiser, G., Ed.; Springer: Berlin, 1982; Vol. 1, pp 305−343.

(19) Clauser, C.; Huenges, E. Thermal conductivity of rocks and minerals, In *A Handbook of Physical Constants, Rock Physics and Phase Relations*; Ahrens, T. J., Ed.; AGU: Washington, DC, 1995; Vol. 3, pp 105−125.

(20) Lebedev, T. S.; Korchin, V. A.; Savenko, B. Ya.; Shapovalov, V. I.; Shepel, S. I. *Physical Properties of Minerals and Matter under PT-Conditions of the Lithosphere*; Academy of Sciences of the Ukraine, Institute of Geophysics: Naukova Dumka, Kiev, 1986.

(21) Volarovich, M. P., Ed. *Physical Properties of Minerals and Rocks at High Thermodynamic Parameters. Handbook*, 2nd ed.; Nedra: Moscow, 1988.

(22) Lebedev, T. S., Ed. *Thermophysical Properties of Rocks*; Nedra: Moscow, 1987.

(23) Lebedev, T. S., Ed. *Petrophysical High PT-Studies and Their Geophysical Applications*; Naukova Dumka: Kiev, 1988.

(24) Amirkhanov, Kh. I.; Emirov, S. N.; Kramynina, N. A. The study of pressure dependence of the thermal conductivity of antimonida of gallium. *Russ. Solid State Phys.* **1983**, *25*, 2486−2492.

(25) Emirov, S. N.; Tsomaeva, T. A.; Askerov, S. Ya. Thermal conductivity of sandstones at high temperatures and high pressures. *Geophysics* **1997**, *19*, 68−75.

(26) Abdulagatov, I. M.; Emirov, S. N.; Tsomaeva, T. A.; Gairbekov, Kh. A.; Askerov, S. Ya. Thermal conductivity of the porous glasses at high temperatures and high pressures. *Russ. High Temp.* **1998**, *36*, 401−409.

(27) Abdulagatov, I. M.; Emirov, S. N.; Tsomaeva, T. A.; Gairbekov, Kh. A.; Askerov, S. Ya.; Magomaeva, M. A. Thermal conductivity of fused quartz and quartz ceramic at high temperatures and high pressures. *J. Phys. Chem. Solids* **2000**, *61*, 779−787.

(28) Abdulagatov, I. M.; Emirov, S. N.; Gairbekov, Kh. A.; Magomaeva, M. A.; Askerov, S. Ya.; Ramazanova, E. N. Effective thermal conductivity of fluid-saturated porous mica ceramics at high temperatures and high pressures. *Ind. Eng. Chem. Res.* **2002**, *41*, 3586−3593.

(29) Seipold, U. The variation of thermal transport properties in the earth's crust. *J. Geodyn.* **1995**, *20*, 145−154.

(30) Seipold, U. Measurements of thermal conductivity and thermal diffusivity of serpentinities at high pressures up to 500 MPa. *High Temp.−High Pressures* **1995/1996**, *27/28*, 147−155.

(31) Birch, F.; Clark, H. The thermal conductivity of rocks and its dependence upon temperature and composition. *Am. J. Sci.* **1940**, *238*, 529−558 and 613−635.

(32) Birch, F. Thermal conductivity and diffusivity. In *Handbook of Physical Constants*; Birch, F., Schairer, F. J., Spicer, H. C., Eds.; Special Paper 36; GSA: New York, 1942; pp 243−266.

(33) Buntebarth, G.; Rueff, P. Laboratory thermal conductivities applied to crustal conditions. *Rev. Bras. Geofis.* **1987**, *5*, 103−109.

(34) Desai, P. D.; Navarro, R. A.; Hasan, S. E.; Ho, C. Y.; DeWitt, D. P.; West, T. R. *Thermophysical Properties of Selected Rocks*; CINDAS Report 23; Center for Information and Numerical Data Analysis and Synthesis (CINDAS), Purdue University: West Lafayette, IN, 1974.

(35) Clark, S. P. Thermal conductivity. In *Handbook of Physical Constants*, Clark, S. P., Ed,; Memoir 97; GSA: New York, 1966; pp 459−482.

(36) Clark, S. P. Heat conductivity in the mantle, in the earth's crust and upper mantle. *Geophys. Monogr. Ser.* **1969**, *No. 13*, 622.

(37) Seipold, U. Simultaneous measurements of thermal diffusivity and thermal conductivity under high pressure using thermal pulses of finite length. *High Temp.−High Pressures* **1988**, *20*, 609−613.

(38) Seipold, U. Pressure and temperature dependence of thermal transport properties for granites. *High Temp.−High Pressures* **1990**, *22*, 541−548.

(39) Seipold, U.; Mueller, H.-J.; Tuisku, P. Principle differences in the pressure dependence of thermal and elastic properties of crystalline rocks. *Phys. Chem. Earth* **1998**, *23*, 357−360.

(40) Seipold, U. Temperature dependence of thermal transport properties of crystalline rocks—a general law. *Tectonophysics* **1998**, *291*, 161−171.

(41) Seipold, U. Investigation of the thermal transport properties of amphibolite. I. Pressure dependence. *High Temp.−High Pressures* **2002**, *34*, 299−306.

(42) Kukkonen, I. T.; Jokinen, J.; Seipold, U. Temperature and pressure dependencies of thermal transport properties of rocks: implications for uncertainties in thermal lithosphere models and new laboratory measurements of high-grade rocs in the central Fennoscandian shield. *Surv. Geophys.* **1999**, *20*, 33−59.

(43) Horai, K.; Susaki, J. The effect of pressure on the thermal conductivity of silicate rocks up to 12 kBar. *Phys. Earth Planet. Int.* **1989**, *55*, 292−305.

(44) Horai, K. Thermal conductivity of rock-forming minerals. *J. Geophys. Res.* **1971**, *76* (5), 1278−1308.

(45) Horai, K. Thermal conductivity of Hawaiian basalt: a new interpretation of Robertson and Peck's data. *J. Geophys. Res.* **1991**, *96*, 4125−4132.

(46) Walsh, J. B.; Decker, E. R. Effect of pressure and saturating fluid on the thermal conductivity of compact rock. *J. Geophys. Res.* **1966**, *71*, 3053−3061.

(47) Anand, J. Thermal conductivity of fluid saturated rocks at elevated pressures and temperatures. M.S. Thesis, University of California, Berkeley, 1971.

(48) Diment, W.; Pratt, H. Thermal conductivity of some rock-forming minerals: a tabulation. *USGS Open File Rep.* **1988**, *No. 690*.

(49) Zierfuss, H.; Viliet, G. V. Laboratory measurements of heat conductivity of sedimentary rocks. *AAPG Bull.* **1956**, *40* (10), 2465−2488.

(50) Edmondson, T. Thermal diffusivity of sedimentary rocks subjected to simulated overburden pressure. M.S. Thesis, University of California, Berkeley, 1961.

(51) Somerton, W. H. *Thermal Properties and Temperature-Related Behavior of Rock/Fluid Systems*; Elsevier: Amsterdam, 1992.

(52) Sorokin, J. A.; Dzavadov, L. N.; Genshaft, J. S. Thermal conductivity of calcite, hornblende and crystalline slate for pressures up to 8 GPa. *Russ. Fiz. Zemli* **1982**, *8*, 88−92.

(53) Tikhomirov, V. Conductivity of rocks and their relationship with density, saturation and temperature. *Russ. Neft. Khoz.* **1968**, *46* (4), 151−161.

(54) Schatz, J. F.; Simmons, G. Thermal conductivity of earth materials at high temperatures. *J. Geophys. Res.* **1972**, *77*, 6966−6983.

(55) Schatz, J. F. Thermal conductivity of earth materials at high temperatures. Ph.D. Thesis, MIT, Cambridge, 1971.

(56) Kristiansen, J. I. The transient cylindrical probe method for determination of thermal parameters of earth materials. *Geoskrifter, Aarhus Univ.* **1982**, *N18*.

(57) Wang, H. F.; Bonner, B. P.; Carlson, S. R.; Kowallis, B. J.; Heard, H. C. Thermal stress cracking in granite. *J. Geophys. Res.* **1989**, *94* (B2), 1742−1758.

(58) Ljubimova, E. A.; Maslennikov, A. I.; Ganijev, Yu. A. Thermal conductivity of dry, wet and oil-saturated rocks at slightly high temperatures and pressures. *Geophys. Res. Bull.* **1977**, *15*, 59−66.

(59) Pribnow, D.; Umsonst, T. Estimation of thermal conductivity from mineral composition: influence of fabric and anisotropy. *Geophys. Res. Lett.* **1993**, *20* (20), 2199−2202.

(60) Pribnow, D.; Williams, C. F.; Burkhardt, H. Log-derived estimate for thermal conductivity of crystalline rocks from the 4 km KTB Vorbohrung. *Geophys. Res. Lett.* **1993**, *20*, 1155−1158.

(61) Pribnow, D.; Sass, J. H. Determination of thermal conductivity from deep boreholes. *J. Geophys. Res.* **1995**, *100*, 9981−9994.

(62) Sass, J. H.; Stone, C.; Munroe, R. J. Thermal conductivity determinations on solid rock-a comparison between a steady-state divided -bar apparatus and a commercial transient line−source device. *J. Volcanol. Geotherm. Res.* **1984**, *20*, 145−153.

(63) Sass, J. H. The thermal conductivity of 15 feldspar specimens. *J. Geophys. Res.* **1965**, *70*, 4064−4065.

(64) Popov, Yu.; Tertychnyi, V.; Bayuk, I.; Korobkov, D. Rock thermal conductivity measurements on core cutting: method and experimental results. In *Proceedings of the International Conference "The Earth's Thermal Field and Related Research Methods"*; MSGPU: Moscow, 2002; pp 223−227.

(65) Popov, Yu.; Romushkevic, R. Thermal conductivity of sedimentary rocks of oil-gas fields. In *Proceedings of the International Conference "The Earth's Thermal Field and Related Research Methods"*; MSGPU: Moscow, 2002; pp 219−223.

(66) Schärli, U.; Rybach, L. On the thermal conductivity of low-porosity crystalline rocks. *Tectonophysics* **1984**, *103*, 307−313.

(67) Huang, J. H. Effective thermal conductivity of porous rocks. *J. Geophys. Res.* **1971**, *76*, 6420−6427.

(68) Beck, A. E. An improved method of computing the thermal conductivity of fluid-filled sedimentary rocks. *Geophysics* **1976**, *41*, 133−144.

(69) Beck, A. E.; Darbha, D. M.; Schloessin, H. H. Lattice conductivities of single-crystal and polycrystalline materials at mantle pressures and temperatures. *Phys. Earth Planet. Int.* **1978**, *17*, 35−53.

(70) Woodside, W.; Messmer, J. Thermal conductivity of porous media. 1. Unconsolidated sands. *J. Appl. Phys.* **1961**, *32* (9), 1688–1699.

(71) Woodside, W.; Messmer, J. Thermal conductivity of porous media. 2. Consolidated rocks. *J. Appl. Phys.* **1961**, *32* (9), 1699–1706.

(72) Mücke, G. *Bergbau Arch.* **1964**, *25*, 35–58.

(73) Ito, Y.; Saito, T.; Nanun, M. *Chinetsu* **1977**, *14*, 21–34.

(74) Kiyohashi, H.; Deguchi, M. Derivation of a correlation formula for the effective thermal conductivity of geological porous materials by three-phase geometric-mean model. *High Temp.–High Pressures* **1998**, *30*, 25–38.

(75) Hofmeister, A. M. Thermal conductivity of spinels and olivines from vibrational spectroscopy: Ambient conditions. *Am. Mineral.* **2001**, *86*, 1188–1208.

(76) Osako, M.; Ito, E.; Yoneda, A. Simultaneous measurements of thermal conductivity and thermal diffusivity for garnet and olivine under high pressure. *Phys. Earth Planet. Int.* **2004**, *143–144*, 311–320.

(77) Osako, M.; Ito, E. Simultaneous thermal diffusivity and thermal conductivity measurements of mantle materials up to 6 GPa. *Rev. High-Pressure Sci. Technol.* **1998**, *7*, 110–112.

(78) Giesting, P. A.; Hofmeister, A. M. Thermal conductivity of disordered garnets from infrared spectroscopy. *Phys. Rev. B* **2002**, *65*, 144305-1-16.

(79) Höfer, M.; Schilling, F. R. Heat transfer in quartz, orthoclase, and sanidine at elevated temperatures. *Phys. Chem. Miner.* **2002**, *29*, 571–584.

(80) Giesting, P. A.; Hofmeister, A. M.; Wopenka, B.; Gwanmesia, G. D.; Jolliff, B. L. Thermal conductivity and thermodynamics of majoritic garnets: implications for the transitions zone. *Earth Planet. Sci. Lett.* **2004**, *218*, 45–56.

(81) Linvill, M. L.; Vandersande, J. W.; Pohl, R. O. Thermal conductivity of feldspars. *Bull Miner.* **1984**, *107*, 521–527.

(82) Cohen, R. E. MgO–the simplest oxide. In *Physics Meets Mineralogy*; Aoki, H., Syono, Y., Hemley, R. J., Eds.; Cambridge University Press: Cambridge, 2000; pp 95–123.

(83) Arndt, J.; Bartel, T.; Scheuber, E.; Schilling F. Thermal and rheological properties of granodioritic rocks from the Central Andes. *Tectonophysics* **1997**, *271*, 75–88.

(84) Blumm, J.; Lemarchand, S. Influence of test conditions on the accuracy of laser flash measurements. *High Temp.–High Pressures* **2002**, *34*, 523–528.

(85) Blumm, J.; Opfermann, J. Improvement of the mathematical modeling of flash measurements. *High Temp.–High Pressures* **2002**, *34*, 515–521.

(86) Xu, Y. S.; Shankland, T. J.; Linhardt, S.; Rubie, D. C.; Langenhorst, F.; Klasinski, K. Thermal diffusivity and conductivity of olivine, wadsleyite and ringwoodite to 20 GPa and 1373 K. *Phys. Earth Planet. Int*. **2004**, *143*, 321–336.

(87) Tommassi, A.; Gibert, B.; Seipold, U.; Mainprice, D. Anisotropy of thermal diffusivity in the upper mantle. *Nature* **2001**, *411*, 783–786.

(88) Chai, M.; Brown, J. M.; Slutsky, L. J. Thermal diffusivity of mantle minerals. *Phys. Chem. Miner.* **1996**, *23*, 470–475.

(89) Roufosse, M.; Klemens, P. G. Lattice thermal conductivity of minerals at high temperature. *J. Geophys. Res.* **1974**, *79*, 703–705.

(90) Höfmeister, A. M. Mantle values of thermal conductivity and the geotherm from phonon lifetimes. *Science* **1999**, *283*, 1699–1706.

(91) Manga, M.; Jeanloz, R. Thermal conductivity of corundum and periclase and implications for the lower mantle. *J. Geophys. Res.* **1997**, *102*, 2999–3008.

(92) Maxwell, J. C. *A Treatise of Electricity and Magnetism*; Clarendon Press: Oxford, 1904; Vol. 1, 435 pp.

(93) Gomma, E. Thermal behavior of partially liquid saturated porous media. Ph.D. Thesis, University of California, Berkeley, 1973.

(94) Ozbek, H. Thermal conductivity of multi-fluid saturated porous media. Ph.D. Thesis, University of California, Berkeley, 1976.

(95) Ghaffari, A. Model for predicting thermal conductivity of rock/fluid systems. Ph.D. Thesis, University of California, Berkeley, 1980.

(96) Odalevskii, V. I. Calculation of the generalized conductivity of heterogeneous systems. *Russ. J. Tech. Phys*. **1951**, *21*, 667–685.

(97) Moyne, C.; Batsale, J. C.; Degiovanni, A.; Maillet, D. Thermal conductivity of wet porous media: theoretical analysis and experimental measurements. In *Thermal Conductivity 21*; Gremers, C. J., Ed.; Plenum Press: New York, 1990; pp 109–115.

(98) Singh, A. K.; Singh, R.; Chaudhary, D. R. Prediction of effective thermal conductivity of moist porous materials. *J. Phys. D: Appl. Phys.* **1990**, *23*, 698–702.

(99) Litovsky, E. Ya.; Shapiro, M. Gas pressure and temperature dependence of thermal conductivity of porous ceramic materials: Part 1, refractoriness and ceramics with porosity below 30 %. *J. Am. Ceram. Soc*. **1992**, *75*, 3425–3431.

(100) Mendel, A. M. Relation between thermal conductivity of rocks and structure of the pores. *Russ. J. Geol. Prospecting* **1997**, *1*, 112–125.

(101) Staicu, D. M.; Jeulin, D.; Beauvy, M.; Laurent, M.; Berlanga, C. Effective thermal conductivity of heterogeneous materials: Calculation methods and application to different microstructures. *High Temp.–High Pressures* **2001**, *23*, 293–301.

(102) Ljubimova, E. A.; Starikova, G. N.; Shushpanov, A. P. Thermophysical studies of rocks. In *Geothermal Studies*; Nauka: Moscow, 1965.

(103) Zoth, G.; Haenel, R. Thermal conductivity. In *Handbook of Terrestrial Heat-Flow Density Determination*; Hänel, R., Rybach, L., Stegena, L., Eds.; Kluwer: Dordrecht, The Netherlands, 1988; pp 449–466.

(104) Ross, R. G.; Anderson, P.; Sundqvist, B.; Bäckström, G. Thermal conductivity of solids and liquids under pressure. *Rep. Prog. Phys.* **1984**, *47*, 1347–1402.

(105) Alm, O.; Bäckström, G. Thermal conductivity of NaCl up to 40 kbar and 240–400 K. *High Temp.–High Pressures* **1975**, *7*, 235–239.

(106) Alm, O.; Bäckström, G. Thermal conductivity of KCl up to 19 kbar. *High Temp.–High Pressures* **1974**, *35*, 421–424.

(107) Bäckström, G. Measurement of thermophysical properties of solids under high pressure. In *Proceedings of the 7th Symposium on Thermophysical Properties*; Cezairliyan, A., Ed.; ASME: New York, 1977; pp 169–180.

(108) Brydsten, U.; Gerlich, D.; Bäckström, G. Thermal conductivity of single-crystal NaCl under uniaxial compression. *J. Phys. C: Solid State Phys.* **1983**, *16*, 143.

(109) Seipold, U.; Schilling, F. R. Heat transport in serpentinites. *Tectonophysics* **2003**, *370*, 147–162.

(110) Seipold, U.; Huenges, E. Thermal properties of gneisses and amphibolites-high pressure and high-temperature investigations of KTB-rock samples. *Tectonophysics* **1998**, *291*, 173–178.

(111) Katsura, T. Thermal diffusivity of olivine under upper mantle conditions. *Geophys. J. Int.* **1995**, *122*, 63–69.

(112) Fujisawa, H.; Fujii, N.; Mizutani, H.; Kanamori, H.; Akimoto, S. Thermal diffusivity of Mg_2SiO_4, Fe_2SiO_4, and NaCl at high pressures and temperatures. *J. Geophys. Res.* **1968**, *73*, 4727–4733.

(113) Ljubimova, E. A.; Maslennikov, A. I.; Ganijev, Yu. A. Thermal conductivity of rocks at high temperatures and high pressures and at oil- and water-saturation. *Russ. Izv. Akad. Nauk SSSR, Ser. Fizika Zemli* **1979**, *9*, 77–82.

(114) Birch, F. The velocity of compressional waves in rocks to 10 kbars. 1. *J. Geophys. Res.* **1960**, *65*, 1083–1102.

(115) Birch, F. The velocity of compressional waves in rocks to 10 kbars. 2. *J. Geophys. Res.* **1961**, *66*, 2199–2224.

(116) Simmons, G. Velocity of shear waves in rocks to 10 kbars. *J. Geophys. Res.* **1964**, *69*, 1123–1130.

(117) Hughes, D. S.; Maurette, C. Elastic wave velocities in granite. *Geophysics* **1956**, *21*, 277–284.

(118) Hughes, D. S.; Maurette, C. Détermination des vitesses d′ondes élastiques dans diverses roches en fonction de la pression et de la temperature. *Rev. Inst. Franc. Petrole Ann. Combust. Liq.* **1957**, *12*, 730–738.

(119) Brace, W. F. Some new measurements of liner compressibility of rocks. *J. Geophys. Res.* **1965**, *70*, 391–398.

(120) Lebedev, T. S.; Shapavalov, V. I. *Temperature Dependence of the Thermal Conductivity Coefficient. Petrophysical Studies at High PT-Conditions*; Nukovo Dumka: Kiev, 1988.

(121) Shimozura, D. Elasticity of rocks and some related geophysical problems. *Jpn. J. Geophys.* **1960**, *2*, 1–85.

(122) Bridgman, P. W. The thermal conductivity and compressibility of several rocks under pressure. *Am. J. Sci.* **1924**, *7*, 81–102.

(123) Powell, R.; Ho, C.; Liley, P. Thermal conductivity of selected materials. *NBS, NS RDS-NBS8*, **1966**.

(124) Clauser, C. Opacity–the concept of radiative thermal conductivity. In *Handbook of Terrestrial Heat Flow Density Determination*; Hanel, R., Rybach, L., Stegena, L., Eds.; Kluwer: Dordrecht, The Netherlands, 1988; pp 143–165.

(125) Eucken, A. Allgemeine gesetzmabigkeiten fuer das warmeleitvermogen verscheidener stoffarten und aggregatzstande. *V. D. I. Forsch.* **1940**, *11*, 6–20.

(126) Szelagowski, H.; Arvanitidis, I.; Seetharaman, S. Effective thermal conductivity of porous strontium oxide and strontium carbonate samples. In *Proceedings of the 5th Asian Thermophysical Properties Conference*, Seoul, Korea; 1998; pp 451–455.

(127) Ziman, J. M. *Electrons and Phonons. The Theory of Transport Phenomena in Solids*; Clarendon Press: Oxford, 1962.

(128) Ratcliffe, E. H. *Brit. J. Appl. Phys.* **1959**, *10*, 22–32.

(129) Scorer, J. Relationship between thermal conductivity and other rocks properties. M.S. Thesis. University of California, Berkeley, 1964.

(130) Williams, C.; Anderson, R. Thermophysical properties of the earth's crust: in situ measurements from continental and ocean drilling. *J. Geophys. Res.* **1990**, *95*, 9209–9236.

Received for review January 11, 2005. Accepted September 29, 2005. This research was supported by Grant RFBR 01-05-64536.

JE050016A